

GW quasiparticle spectra from occupied states only

P. Umari,¹ Geoffrey Stenuit,¹ and Stefano Baroni^{2,1}

¹*INFN-CNR DEMOCRITOS Theory@Elettra Group, c/o Sincrotrone Trieste, Area Science Park, Basovizza, I-34012 Trieste, Italy*

²*SISSA—Scuola Internazionale Superiore di Studi Avanzati, via Beirut 2-4, Grignano, I-34151 Trieste, Italy*

(Received 5 October 2009; revised manuscript received 4 January 2010; published 3 March 2010)

We introduce a method that allows for the calculation of quasiparticle spectra in the GW approximation, yet avoiding any explicit reference to empty one-electron states. This is achieved by expressing the irreducible polarizability operator and the self-energy operator through a set of linear response equations, which are solved using a Lanczos-chain algorithm. We first validate our approach by calculating the vertical ionization energies of the benzene molecule and then show its potential by addressing the spectrum of a large molecule such as free-base tetraphenylporphyrin.

DOI: [10.1103/PhysRevB.81.115104](https://doi.org/10.1103/PhysRevB.81.115104)

PACS number(s): 71.15.Qe, 31.15.xm, 71.15.Mb

I. INTRODUCTION

In spite of the formidable success met over the past forty years in the simulation of materials, based on electronic-structure theory,¹ density-functional theory (DFT) (Ref. 2) is essentially limited to ground-state properties and its time-dependent extension³ still displays conceptual and practical difficulties. Many-body perturbation theory (MBPT),⁴ in turn, provides a general, though awkward, framework for simulating electronic excitation processes in materials. The most elementary such process is the removal/addition of an electron from a system originally in its ground state. These processes are accessible to direct/inverse photoemission spectroscopies and can be described theoretically in terms of *quasiparticle* (QP) spectra.⁴ A numerically viable approach to QP energy levels [known as the GW approximation, (GWA)] was introduced in the 60s,^{5,6} but it took two decades for a realistic application of it to appear,⁷ and still now the routine application of MBPT to the simulation of materials is plagued by severe numerical difficulties, which have limited so far these applications to models of a few handfuls of non-equivalent atoms, at most. The two main such difficulties are the necessity to calculate and manipulate large matrices representing the charge response of the system (electron polarizabilities or polarization propagators),⁸ on the one hand, and that of expressing such response functions in terms of slowly converging sums over empty one-electron states,^{8–11} on the other hand. Indeed, well converged sums cannot be obtained but for very small systems/simulation cells. In a recent paper, we have successfully addressed the first problem by expressing polarizability operators in terms of an optimally small set of basis functions.⁸ In the present article we address, and hopefully solve, the second problem by introducing in Sec. II a method¹² to calculate polarizability operators and self-energy operators, based on a Lanczos-chain technique, inspired by recent progresses in time-dependent density-functional perturbation theory.^{13,14} In the same section, we explain how also optimal basis sets for representing polarizability matrices can be obtained without calculating empty states. In Sec. III we validate our approach by calculating the vertical ionization energies of the benzene molecule, and demonstrate its power by addressing the spectrum of a large molecule such as free-base tetraphenylporphyrin. Finally, the conclusions are drawn in Sec. IV.

II. METHOD

QP energies (QPE) are eigenvalues of a Schrödinger-like QP equation (QPEq) for the so-called QP amplitudes (QPA), which is similar to the DFT Kohn-Sham equation with the exchange-correlation potential, $V_{xc}(\mathbf{r})$, replaced by the non-local, energy dependent, and non-Hermitian self-energy operator, $\Sigma(\mathbf{r}, \mathbf{r}', \omega)$. In the GWA (Refs. 5 and 6) Σ is the convolution of the one-electron propagator, G , and of the dynamically screened interaction, W :

$$\Sigma_{GW}(\mathbf{r}, \mathbf{r}'; \omega) = \frac{i}{2\pi} \int_{-\infty}^{\infty} d\omega' G(\mathbf{r}, \mathbf{r}'; \omega') W(\mathbf{r}, \mathbf{r}'; \omega - \omega'), \quad (1)$$

where $W = v + v \cdot \Pi \cdot v$, $\Pi(\mathbf{r}, \mathbf{r}'; \omega) = (1 - P \cdot v)^{-1} \cdot P$ is the reducible polarizability, P the irreducible one, $v(\mathbf{r}, \mathbf{r}') = \frac{1}{|\mathbf{r} - \mathbf{r}'|}$ is the bare Coulomb interaction, and a dot indicates the product of two kernels such as in $v \cdot \Pi(\mathbf{r}, \mathbf{r}'; \omega) = \int d\mathbf{r}'' v(\mathbf{r}, \mathbf{r}'') \Pi(\mathbf{r}'', \mathbf{r}'; \omega)$. We assume time-reversal invariance to hold—so that wave-functions are real—and we work on the imaginary-frequency axis;¹⁵ real-frequency results are then recovered upon analytic continuation. One further approximation is the so-called $G^{\circ}W^{\circ}$ one, where the one-electron propagator is obtained from the QPEq using a model real and energy-independent self-energy, such as, e.g., $\Sigma^{\circ} = V_{xc}(\mathbf{r}) \delta(\mathbf{r} - \mathbf{r}')$, and the irreducible polarizability is calculated in the random-phase approximation (RPA)

$$P^{\circ}(\mathbf{r}, \mathbf{r}'; i\omega) = 4 \operatorname{Re} \sum_{cv} \frac{\psi_c(\mathbf{r}) \psi_v(\mathbf{r}') \psi_v(\mathbf{r}) \psi_c(\mathbf{r}')}{i\omega - (\epsilon_c - \epsilon_v)}, \quad (2)$$

where ψ and ϵ are zeroth order QPAs and QPEs and v and c suffixes indicate occupied and empty states, respectively. To first order in $\hat{\Sigma}' = \hat{\Sigma}_{G^{\circ}W^{\circ}} - \hat{\Sigma}^{\circ}$, QPEs are given by the equation: $E_n \approx \epsilon_n + \langle \hat{\Sigma}_{G^{\circ}W^{\circ}}(E_n) \rangle_n - \langle \hat{V}_{xc} \rangle_n$, where $\langle \hat{A} \rangle_n = \langle \psi_n | \hat{A} | \psi_n \rangle$, and quantum-mechanical operators are indicated by a caret.

In Ref. 8, we reported on a strategy to build an optimal representation for the polarizability operators, in terms of a reduced, yet controllable accurate, orthonormal basis set $\{\Phi_{\mu}(\mathbf{r})\}$

$$P^\circ(\mathbf{r}, \mathbf{r}', i\omega) = \sum_{\mu\nu} P_{\mu\nu}^\circ(i\omega) \Phi_\mu(\mathbf{r}) \Phi_\nu(\mathbf{r}'). \quad (3)$$

Using the RPA, Eq. (2), $P_{\mu\nu}^\circ(i\omega)$ reads

$$P_{\mu\nu}^\circ(i\omega) = -4 \operatorname{Re} \sum_{v,c} \frac{1}{\epsilon_c - \epsilon_v + i\omega} \times \int d\mathbf{r} d\mathbf{r}' \Phi_\mu(\mathbf{r}) \psi_v(\mathbf{r}) \psi_c(\mathbf{r}) \psi_v(\mathbf{r}') \psi_c(\mathbf{r}') \Phi_\nu(\mathbf{r}'). \quad (4)$$

Suppose that such a representation for P° can be found without any explicit reference to empty states (later we will show how this can be achieved). In order to eliminate the sum over empty states in Eq. (4), we introduce the projector operator over the empty-state (*electron*) manifold, $\hat{Q}_e = \hat{1} - \hat{Q}_h$, \hat{Q}_h being the projector onto occupied (*hole*) states. In terms of \hat{Q}_e , Eq. (4) reads

$$P_{\mu\nu}^\circ(i\omega) = -4 \operatorname{Re} \sum_v \langle \psi_v \Phi_\mu | \hat{Q}_e (\hat{H}^\circ - \epsilon_v + i\omega)^{-1} \hat{Q}_e | \psi_v \Phi_\nu \rangle, \quad (5)$$

where \hat{H}° is the QP Hamiltonian corresponding to $\hat{\Sigma}^\circ$ and $|\psi_v \Phi_\nu\rangle$ is the vector whose coordinate representation is $\langle \mathbf{r} | \psi_v \Phi_\nu \rangle = \psi_v(\mathbf{r}) \Phi_\nu(\mathbf{r})$. A direct approach to Eq. (5) would require the inversion of $(\hat{H}^\circ - \epsilon_v + i\omega)$ for every value of the (imaginary) frequency and the application of the resulting inverse to $N_v \times N_p$ vectors, where N_v and N_p are the number of valence states and polarizability basis functions, respectively, thus making the resulting algorithm unwieldy.

In order to substantially reduce the computational load, we proceed in two steps: we first reduce the number of functions to which the inverse shifted Hamiltonian in Eq. (5) has to be applied; in the second step, the inversion of the shifted Hamiltonian is avoided by a Lanczos-chain algorithm that need not to be repeated for different values of the (imaginary) frequency shift. In the first step an approximate orthonormal basis, $\{t_\alpha(\mathbf{r})\}$, is built for the linear space spanned by the $N_v \times N_p$ vectors, $\{\hat{Q}_e |\psi_v \Phi_\mu\rangle\}$:

$$\Psi_{v\mu}(\mathbf{r}) \doteq \langle \mathbf{r} | \hat{Q}_e |\psi_v \Phi_\mu\rangle \approx \sum_{\alpha=1}^{N_T} t_\alpha(\mathbf{r}) T_{\alpha,v\mu}, \quad (6)$$

where $T_{\alpha,v\mu} = \langle t_\alpha | \hat{Q}_e |\psi_v \Phi_\mu\rangle$ and N_T is the number of t functions, which can be kept in general significantly smaller than $N_v \times N_p$. The most general way to achieve this goal is to perform a singular-value decomposition of the Ψ s and to keep only those linear combinations of them that correspond to a singular value larger than a given threshold. For numerical convenience, we prefer here to adopt a different three-step procedure. In the first step we express the ψ s in terms of maximally localized Wannier functions,¹⁶ $\{w_l(\mathbf{r})\}$, and we define the corresponding product functions as $\bar{\Psi}_{l\mu}(\mathbf{r}) = \langle \mathbf{r} | \hat{Q}_e | w_l \Phi_\mu \rangle$ (Ψ s are linear combinations of $\bar{\Psi}$ s, so that a basis for the latter would also be a basis for the former). In the second step, for each given value of l , we calculate and

keep the eigenstates of the overlap matrix $S_{\mu\nu}^l = \langle \bar{\Psi}_{l\mu} | \bar{\Psi}_{l\nu} \rangle$, whose eigenvalue is larger than a given threshold⁸ (the number of such significant eigenvalues depends in general on l , but for simplicity we keep an equal number of them for all l s, say m). The advantage of passing to the Wannier representation is that this transformation reduces the number of significant eigenvalues of the overlap matrix. The procedure outlined so far results in N_v blocks of m orthonormal functions, which span the original manifold of the Ψ s. Functions belonging to different blocks are not orthogonal. The third step consists in a Gram-Schmidt orthonormalization across different blocks. Once the first block is generated, each of the next ones is orthogonalized on the fly to all of the previous blocks. The resulting functions are no longer orthonormal. A minimal orthonormal basis is finally generated as above by diagonalizing the corresponding overlap matrix and retaining only those eigenvectors that correspond to eigenvalues larger than a given threshold.⁸

Once a basis for the manifold spanned by the Ψ s have been thus generated, using Eqs. (5) and (6), Eq. (4) reads

$$P_{\mu\nu}^\circ(i\omega) \approx -4 \operatorname{Re} \sum_{v,\alpha\beta} \langle t_\alpha | (\hat{H}^\circ - \epsilon_v + i\omega)^{-1} | t_\beta \rangle \times T_{\alpha,v\mu} T_{\beta,v\nu}. \quad (7)$$

Having thus reduced the number of matrix elements of the resolvent of the Hamiltonian in Eq. (5), these matrix elements can be efficiently calculated by a Lanczos-chain algorithm,¹⁷ as explained in Ref. 14. In a nutshell, a frequency-independent Lanczos chain of vectors is generated, starting from each one of the t functions. In the basis of each one of these chains the Hamiltonian is tridiagonal and thus easily inverted.

A similar approach can be applied to the calculation of the expectation values of the self-energy. By expressing the reducible polarizability in the same representation used for the irreducible one, Eq. (3), $\Pi(\mathbf{r}, \mathbf{r}', \omega) = \sum_{\mu\nu} \Pi_{\mu\nu}(\omega) \Phi_\mu(\mathbf{r}) \Phi_\nu(\mathbf{r}')$, the diagonal matrix elements of the correlation contribution $\hat{\Sigma}_c$ to the self-energy, Eq. (1), can be cast into the form:

$$\langle \hat{\Sigma}_c(i\omega) \rangle_n = \frac{1}{2\pi} \sum_{\mu,\nu} \int d\omega' \Pi_{\mu\nu}(i\omega') \times \langle \psi_n(v\Phi_\mu) | (\hat{H}^\circ - i(\omega - \omega'))^{-1} | \psi_n(v\Phi_\nu) \rangle, \quad (8)$$

where $|\psi_n(v\Phi_\mu)\rangle$ is the vector whose coordinate representation reads $\langle \mathbf{r} | \psi_n(v\Phi_\mu) \rangle = \psi_n(\mathbf{r}) \int v(\mathbf{r}, \mathbf{r}') \Phi_\mu(\mathbf{r}') d\mathbf{r}'$. The matrix elements on the right-hand side of Eq. (8) are calculated with a similar procedure as for Eq. (5), where the set of vectors $\{|\psi_n(v\Phi_\mu)\rangle\}$ is first expanded into a suitable optimal basis set, $\{s_\alpha(\mathbf{r})\}$

$$\langle \mathbf{r} | \psi_n(v\Phi_\mu) \rangle \approx \sum_{\alpha=1}^{N_S} s_\alpha(\mathbf{r}) S_{\alpha,n\mu}, \quad (9)$$

and then by generating a Lanczos chain for each s ; the convolution is finally calculated either by direct integration or by fast Fourier transform.

In Ref. 8 a reduced basis set for the polarizability operators was constructed by expressing the product functions, $\psi_c(\mathbf{r})\psi_v(\mathbf{r})$, in Eq. (2) in terms of localized Wannier-like orbitals. Although the number of empty states needed to achieve a good accuracy can be kept fairly small, still quite a few of them have to be calculated. On the other hand, it was noted that this basis can be kept independent on frequency (or on time). An optimal representation for the polarizability can be thus calculated by diagonalizing the irreducible polarizability operator at $t=0$ and keeping only those eigenvectors that correspond to eigenvalues larger than a certain threshold. One has

$$\begin{aligned} P^o(\mathbf{r}, \mathbf{r}'; t=0) &= \sum_{cv} \psi_c(\mathbf{r})\psi_v(\mathbf{r})\psi_c(\mathbf{r}')\psi_v(\mathbf{r}') \\ &= Q_h(\mathbf{r}, \mathbf{r}')Q_e(\mathbf{r}, \mathbf{r}'), \end{aligned} \quad (10)$$

where Q_h and Q_e are real-space representations of the projectors onto the hole and electron manifolds, respectively. The eigenpairs of $P^o(t=0)$ can be easily calculated by iterative diagonalization, noting that $Q_e(\mathbf{r}, \mathbf{r}') = \delta(\mathbf{r}-\mathbf{r}') - Q_h(\mathbf{r}, \mathbf{r}')$. Such a procedure would lead however to a number of eigenpairs much larger than strictly needed to achieve a good accuracy in the QP spectra. In order to keep the size of the polarizability basis manageable, we replace \hat{Q}_e in Eq. (10) with the projector over the manifold spanned by plane waves (PWs) up to a kinetic energy of E^* , orthogonalized to the hole manifold [*orthogonalized plane waves* (OPWs)], \hat{Q}_e^* . Let $|\bar{\mathbf{G}}\rangle = \hat{Q}_e^*|\mathbf{G}\rangle$ be one such OPW. In terms of the OPWs, the modified projector reads:

$$\hat{Q}_e^* = \sum_{|\mathbf{G}|^2, |\mathbf{G}'|^2 \leq E^*} |\bar{\mathbf{G}}\rangle \langle \bar{\mathbf{G}}'| \times S_{\mathbf{G}\mathbf{G}'}, \quad (11)$$

where $S_{\mathbf{G}\mathbf{G}'} = \langle \bar{\mathbf{G}} | \bar{\mathbf{G}}' \rangle$. Using this approximation, a basis for the polarizability can be obtained from the eigenfunctions of the eigenvalue equation:

$$\sum_v \psi_v(\mathbf{r}) \langle \mathbf{r} | \hat{Q}_e^* | \psi_v \Phi_\mu \rangle = q_\mu \Phi_\mu(\mathbf{r}), \quad (12)$$

whose leading eigenpairs—corresponding to eigenvalues larger than a given threshold, q^* —can be easily found by conjugate gradients or other iterative methods.¹⁷ We stress that this is a controlled approximation, which can be systematically improved; furthermore, it only affects the determination of an optimal representation for the polarizability operators, not their actual calculation once this basis has been determined.

III. BENCHMARK AND APPLICATIONS

Our scheme has been implemented for norm-conserving pseudopotentials (PPs) in the `gww.x` module of the QUANTUM ESPRESSO distribution of electronic-structure codes,¹⁸ soon to be released under the GPL license, and benchmarked on the isolated benzene molecule.¹⁹ In Fig. 1 we display the vertical ionization potential (VIP) calculated for the isolated benzene (C_6H_6) molecule with different values of the energy and eigenvalue cutoffs, E^* and q^* , defining the polarizability

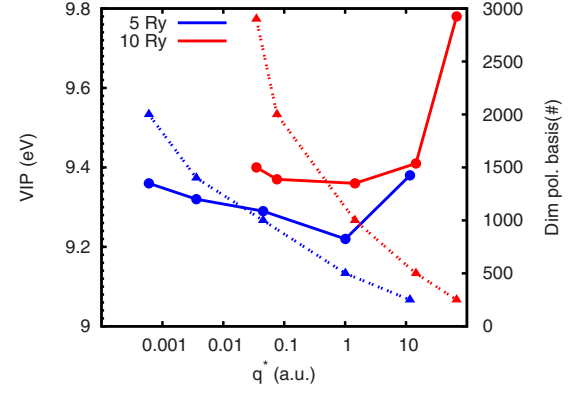


FIG. 1. (Color online) Calculated vertical ionization potential of the benzene molecule (disks, left scale) and dimension of the polarizability basis (triangles, right scale) versus the q^* cutoff in atomic units. The polarizability basis sets have been constructed with energy cutoffs: $E^*=5$ Ry blue (black) and $E^*=10$ Ry red (gray). The lines are a guide to the eye.

basis [see Eqs. (11) and (12)]. The two series of calculations for $E^*=5$ and 10 Ry converge to the same VIP within few tens of meV. For both values of E^* , a cutoff $q^* \sim 10$ a.u. yields convergence within ~ 0.1 eV, which is our estimated residual accuracy due to the uncertainties of the analytical continuation procedure. The convergence of the VIP with respect to the size of the polarizability basis is slightly slower here than previously observed in Ref. 8, where sums over empty states were performed explicitly including a limited number of them. In Fig. 2 we display the differences between the calculated and experimental VIPs in benzene ($E^*=10$ Ry, $q^*=0.035$ a.u., corresponding to ~ 2900 basis functions). On the same figure we also report results obtained: (i) with a reduced polarizability basis ($E^*=10$ Ry,

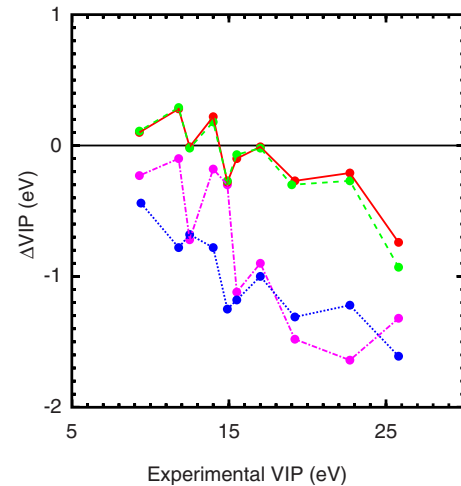


FIG. 2. (Color online) Differences between the calculated VIPs of benzene and experimental results. Red (solid) and green (dashed): present method using $E^*=10$ Ry, $q^*=0.035$ a.u. and $E^*=10$ Ry, $q^*=14.5$ a.u., respectively. Magenta (dot dashed): method of Ref. 8, upon extrapolation of the sum over virtual states. Blue (dotted): present method, but using a polarizability basis formed by PWs (see text). Experimental data are from Ref. 21. The lines are a guide to the eye.

$q^* = 14.5$ a.u. corresponding to ~ 500 basis functions); (ii) with the extrapolation of the sum over virtual orbitals described in Ref. 8; (iii) with a polarizability basis of ~ 1500 PWs (corresponding to a kinetic-energy cutoff of 5 Ry). Not unexpectedly, GW results are in good agreement with experiment. GW calculations based on explicit sums over empty states could hardly converge for simulation cells/basis sets of this size, thus requiring suitable extrapolation.⁸ Avoiding any such extrapolations our method enhances both the accuracy and the speed²² of the calculation. We also found, as expected, that the calculations converge faster with respect to the size of the polarizability basis using the optimal polarizability basis method than using simple PW basis sets.

We now demonstrate the potential of our method by considering the free-base tetraphenylporphyrin molecule (TPPH₂) (C₄₄H₃₀N₄).¹⁹ We used a polarizability basis of 5000 elements, which has been obtained from Eq. (12) using $E^* = 10$ Ry and $q^* = 21.1$ a.u. These parameters ensure an absolute convergence of the calculated QPEs of ~ 0.1 eV. We note that the analytic continuation procedure involves uncertainties of similar size or even larger for the lowest lying states. The calculated ionization potential is 6.7 eV, in fair agreement with an experimental value of 6.4 eV.²³ The quality of our results is further illustrated in Fig. 3, where we compare the calculated valence electronic density of states with photoemission data from Ref. 23. Nice agreement is achieved for the position of the peaks, while the agreement for the intensities is not as good, possibly due to our neglect of any matrix-element effect.

IV. CONCLUSIONS

In conclusion, we believe that the method presented here may open the way to *ab initio* MBPT simulations of large

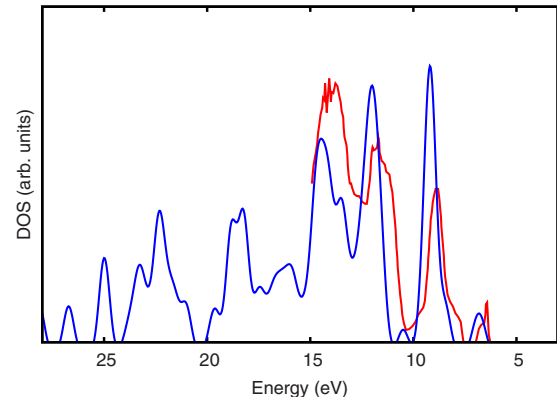


FIG. 3. (Color online) Valence electronic density of states for the TPPH₂ molecule, blue (black): theory (a Gaussian broadening of 0.25 eV has been used); red (gray): photoemission data from Ref. 23.

and realistic models of molecular and nanostructured, as well as to more standard crystalline systems.²⁴ While we feel that the proposed Lanczos technique may be considered as a sort of definitive answer to the sum-over-virtual-states problem, we think that there is still room for improving the construction of an optimal polarizability basis. The extension of these ideas to real-frequency implementations of GW and other MBPT techniques, such as the Bethe-Salpeter equation, is possible, and indeed presently under way.

ACKNOWLEDGMENTS

P.U. thanks Xiaofeng Qian and Nicola Marzari for useful discussions and the latter for hospitality at MIT. The calculations were performed using the computational facilities of CINECA.

¹See, e.g., R. M. Martin, *Electronic Structure* (Cambridge University Press, Cambridge, 2004) and references quoted therein.

²P. Hohenberg and W. Kohn, *Phys. Rev.* **136**, B864 (1964); W. Kohn and L. J. Sham, *ibid.* **140**, A1133 (1965).

³E. Runge and E. K. U. Gross, *Phys. Rev. Lett.* **52**, 997 (1984); M. A. L. Marques, C. L. Ullrich, F. Nogueira, A. Rubio, K. Burke, and E. K. U. Gross, *Time-Dependent Density Functional Theory, Lecture Notes in Physics* (Springer-Verlag, Berlin, Heidelberg, 2006), Vol. 706.

⁴L. Hedin and S. Lundqvist, in *Solid State Physics, Advances in Research and Application*, edited by F. Seitz, D. Turnbull, and H. Ehrenreich (Academic, New York, 1969), Vol. 23, p. 1.

⁵L. Hedin, *Phys. Rev.* **139**, A796 (1965).

⁶F. Aryasetiawan and O. Gunnarsson, *Rep. Prog. Phys.* **61**, 237 (1998).

⁷M. S. Hybertsen and S. G. Louie, *Phys. Rev. Lett.* **55**, 1418 (1985).

⁸P. Umari, G. Stenuit, and S. Baroni, *Phys. Rev. B* **79**, 201104(R) (2009).

⁹L. Reining, G. Onida, and R. W. Godby, *Phys. Rev. B* **56**, R4301 (1997).

¹⁰L. Steinbeck, A. Rubio, L. Reining, M. Torrent, I. D. White, and R. W. Godby, *Comput. Phys. Commun.* **125**, 105 (2000).

¹¹F. Bruneval and X. Gonze, *Phys. Rev. B* **78**, 085125 (2008).

¹²Recently, F. Giustino and co-workers also reported on a method for performing GW calculations without calculating any empty state. They implemented it as a proof of concept within the empirical pseudopotential formalism. [F. Giustino, M. L. Cohen, and S. G. Louie, *Phys. Rev. B* **81**, 115105 (2010).]

¹³B. Walker, A. M. Saitta, R. Gebauer, and S. Baroni, *Phys. Rev. Lett.* **96**, 113001 (2006).

¹⁴D. Rocca, R. Gebauer, Y. Saad, and S. Baroni, *J. Chem. Phys.* **128**, 154105 (2008).

¹⁵H. N. Rojas, R. W. Godby, and R. J. Needs, *Phys. Rev. Lett.* **74**, 1827 (1995); M. M. Rieger, L. Steinbeck, I. D. White, H. N. Rojas, and R. W. Godby, *Comput. Phys. Commun.* **117**, 211 (1999).

¹⁶N. Marzari and D. Vanderbilt, *Phys. Rev. B* **56**, 12847 (1997).

¹⁷See, e.g., Y. Saad, *Iterative Methods for Sparse Linear Systems*, 2nd ed. (SIAM, Philadelphia, 2003).

¹⁸P. Giannozzi *et al.*, *J. Phys.: Condens. Matter* **21**, 395502 (2009); <http://www.quantum-espresso.org>.

¹⁹PPs H.pz-vbc.UPF, C.pz-vbc.UPF, and N.pz-vbc.UPF from the QUANTUM ESPRESSO distribution were used with PW kinetic-energy cutoff of 40 and 45 Ry for C₆H₆ and TPPH₂, respectively. For C₆H₆ we used a cubic supercell of 20 a.u. edge, while for TPPH₂ an orthorhombic cell of 37.8×37.8×26.5 a.u. was used. In all cases, an imaginary-frequency cutoff of 40 Ry, frequency grids of 200 equally spaced points on each half frequency axis and 20 Lanczos steps were used. We imposed that Eqs. (6) and (9) were satisfied to 99.8% for C₆H₆ and to 98.6% for TPPH₂, assuring the convergence of the calculated QPEs for a given polarizability basis within 0.01 eV and 0.03 eV, respectively, and requiring from ~900 to ~3000*t* and from ~800 to ~2000*s* functions for C₆H₆ and ~9600*t* and ~4300*s* functions for TPPH₂. In order to avoid spurious interactions with periodic replicas of the molecule, a cutoff was applied to the Coulomb interaction as explained, e.g., in Ref. 20.

²⁰G. Onida, L. Reining, R. W. Godby, R. Del Sole, and W. Andreoni, Phys. Rev. Lett. **75**, 818 (1995).

²¹C. Fridh, L. Åsbrink, and E. Lindholm, Chem. Phys. Lett. **15**, 282 (1972).

²²The present Lanczos method allowed us to calculate the GW spectrum of C₆H₆ using a polarizability basis of 500 elements in a time which was ≈1/10 that needed by extrapolating sums-over-virtual-states of 1000, 2000, and 3000 virtual terms. The convergence of this sum is so slow that fully converged results could not be obtained in this case.

²³N. E. Gruhn, D. L. Lichtenberger, H. Ogura, and F. A. Walker, Inorg. Chem. **38**, 4023 (1999).

²⁴For extended systems, the long-range terms arising in the GW formalism can also be calculated using optimal basis sets and Lanczos chains.